Anal Bioanal Chem (2012) 402:2385–2393
DOI 10.1007/s00216-012-5736-x

SHORT COMMUNICATION

Glucose sensitive poly (*N*-isopropylacrylamide) microgel based etalons

Courtney D. Sorrell · Michael J. Serpe

Received: 11 October 2011 / Revised: 19 December 2011 / Accepted: 10 January 2012 / Published online: 28 January 2012

Abstract Thermoresponsive microgels have been shown to be an excellent platform for designing sensor materials. Recently, poly (*N*-isopropylacrylamide)-*co*-acrylic acid (pNIPAm-*co*-AAc) microgel based etalon materials have been described as direct sensing materials that can be designed to have a single, unique color. These color tunable materials show immense promise for sensing due to their spectral sensitivity and bright visual color. Here, we describe a *proof-of-concept* for etalon sensing of glucose. We found that aminophenylboronic acid (APBA)-functionalized pNIPAm-*co*-AAc microgels in an etalon respond to 3 mg/mL glucose concentrations by red shifting their reflectance peaks by 110 nm up to 150 nm. Additionally, APBA-functionalized pNIPAm-*co*-AAc microgels have a depressed volume phase transition temperature at 18–20 °C, which shifts to 24–26 °C after glucose binding. We also demonstrate that these materials show a marked visual color change, which is a first step towards developing direct read-out sensor devices.

Keywords Poly (*N*-isopropylacrylamide) microgels · Color tunable materials · Fabry–Pérot etalon · Stimuli responsive polymers · Metal–polymer hybrid structures · Glucose sensing

Abbreviations

AAc	acrylic acid
APBA	3-aminophenylboronic acid
BIS	*N,N′*-methylenebisacrylamide
D_H	hydrodynamic diameter
EDC	1-ethyl-3-(3-dimethylaminopropyl)carbodiimide
NIPAm	*N*-isopropylacrylamide
PCS	photon correlation spectroscopy
pNIPAm	poly (*N*-isopropylacrylamide)
POC	point-of-care
VPTT	volume phase transition temperature

Introduction

Point-of-care (POC) diagnostics are extremely important and desirable in economically strained regions and developing nations because they are often inexpensive, portable, simple to manufacture, and require little to no sample preparation and training to use [1–3]. Many portable POC devices also feature direct "read-out" capabilities, which do not require a spectrometer or other piece of expensive laboratory equipment to determine the test result [4, 5]. Sensors of this type have broad applicability and have been developed for drug screening [5] and to detect blood glucose levels [6], early pregnancy [7], and various disease biomarkers [8, 9]. Detection of these analytes often requires a sensitive device that can distinguish an analyte from within a complex solution; therefore, new materials are in development in order to enhance diagnostic sensing. Of particular interest is the need to measure elevated glucose concentrations in blood and other bodily fluids, which is becoming a growing health concern for a large portion of the population.

Electronic supplementary material The online version of this article (doi:10.1007/s00216-012-5736-x) contains supplementary material, which is available to authorized users.

C. D. Sorrell · M. J. Serpe (✉)
Department of Chemistry, University of Alberta,
11227 Saskatchewan Drive,
Edmonton, Alberta, Canada T6G 2G2
e-mail: michael.serpe@ualberta.ca

While there are many options for monitoring glucose, new materials that can perform this task are always needed. Glucose monitoring is also a useful model system to identify new materials and devices for bioanalytical applications [6, 10–12].

Microgels are colloidally stable hydrogel particles. Poly (*N*-isopropylacrylamide) (pNIPAm) microgels are a class of materials that are referred to as thermoresponsive. Specifically, thermoresponsive pNIPAm microgels undergo a volume phase transition from a swollen to a collapsed state at ~32 °C, which results in a decrease in microgel diameter [13–15]. Microgels can be synthesized with a co-monomer like acrylic acid (AAc) to provide additional responsivity, such as to changes in pH, or for a chemical handle for further microgel functionalization, such as for carbodiimide coupling reactions [16].

Glucose sensitive gels, microgels, and colloidal crystal arrays have been previously studied and characterized by several research groups [6, 10, 11, 17–19]. Microgels offer a unique platform for building sensing materials because of their small size and easy processing for fabrication of coatings and films [20, 21], layer-by-layer structures [22, 23], and 3D optical materials [24, 25]. Other researchers have shown that microgels functionalized with 3-aminophenylboronic acid (APBA) respond to small changes in glucose concentration by swelling (increasing diameter), which can be measured by photon correlation spectroscopy (PCS) [17, 18]. The swelling response is driven by both the Donnan equilibrium of the charged species in the gel and Coulombic repulsion of the negative charges on the hydroxylated boron. They also found that APBA-functionalized microgels that have not been exposed to glucose exhibit a lower volume phase transition temperature (VPTT) than unmodified pNIPAm-*co*-AAc microgels. They attribute these changes in the physical behavior of the microgels to an increase in the hydrophobicity of the hydrogel backbone due to the addition of the phenyl group of the boronic acid moiety on the acrylic acid comonomer. The binding of glucose to the APBA increases the charge density inside the microgel and causes it to swell, but the hydrophobicity of the polymer at elevated temperature can still overcome the increased Coulombic repulsion inside the gel, which results in an increase in the VPTT towards 32 °C expected for pNIPAm [17, 18].

A Fabry–Pérot etalon/interferometer, or "etalon", is an optical device that consists of a dielectric layer between two reflective mirrors [26, 27]. When light impinges on an etalon, some passes into the dielectric cavity, where constructive/destructive light interference occurs. This interference enhances certain wavelengths of light, while others are diminished, which is exhibited as a spectrum, with multiple peaks at wavelength positions dictated by the following equation:

$$\lambda m = 2nd\cos\theta \quad (1)$$

where λ is the wavelength maximum of the peak(s), m is the peak order (e.g., 1,2,3,….), n is the refractive index of the dielectric, d is the spacing between the mirrors, and θ is the angle of incidence [27]. Because λ is directly proportional to n, an increase in n for a given peak of order m results in a red shift. Similarly, because λ is also proportional to the distance between the two mirrors, d, an increase in d gives rise to a red shift for the peak, λ.

Our group generates color tunable materials by sandwiching pNIPAm-*co*-AAc microgels between two thin gold (Au) films resulting in the "mirror-dielectric-mirror" configuration of an etalon [28–30]. These microgel etalons can be fabricated to have a single bright color [30], and because the microgels exhibit a diameter that is dependent on temperature and pH, the mirror–mirror spacing can be tuned resulting in a color change according to Eq. (1) [28–30]. These materials exhibit multi-peak spectra that shift spectrally in response to an increase in temperature, ca. 300 nm blue shift as the solution temperature is increase from 25 °C to 40 °C. This high sensitivity makes microgel based etalons excellent platforms for optical sensing applications. By incorporating analyte sensitive microgels into the etalon, the mirror-mirror distance will depend on the presence or absence of a specific analyte, such as glucose. To develop such sensors, it is important to understand the mechanism by which microgel etalons actuate. We recently described a kinetics model for microgel etalons that indicate that a thin Au overlayer (around 5 nm, with a 2-nm Cr adhesion layer) is ideal for minimizing the response time required for a change in the solvation state of the etalon, and we feel that this type of device would be ideal for colorimetric POC sensing [30, 31].

Herein, we demonstrate the utility of microgel based etalons for sensing applications. Using APBA-functionalized microgel etalons, we are able to detect glucose both visually and spectrally. Spectrally, the etalon's reflectance peaks red shift in response to glucose addition, yielding a visible color change. APBA is not specific for glucose, as it can bind to other diols non-specifically, the purpose of this manuscript is to demonstrate that biologically relevant molecules (glucose) can enter the etalon, interact with the APBA-modified microgels, and afford a colorimetric and spectral response. Previously, dispersed APBA-functionalized microgels were shown to swell in the presence of glucose, [17, 18] but it is unclear how they respond in devices that are able to produce a readout signal—this study shows that the APBA microgels function in our devices as expected from their solution behavior. This is very important for future studies in the group, but also shows that confined, functional microgels can interact with their environment for sensing applications.

Experimental

Materials *N*-isopropylacrylamide was purchased from TCI (Portland, Oregon) and purified by recrystallization from

hexanes (ACS reagent grade, EMD, Gibbstown, NJ) prior to use. *N,N′*-methylenebisacrylamide (BIS; 99%), acrylic acid (AAc; 99%), ammonium persulfate (APS; 98+%), α-D-glucose (ACS reagent), and APBA hydrochloride (98%) were obtained from Sigma-Aldrich (Oakville, Ontario, Milwaukee, WI, and St. Louis, MO) and were used as received. Sodium chloride and sodium phosphate monobasic were obtained from Fisher (Ottawa, Ontario) and used as received. Sodium bicarbonate ($NaHCO_3$) and sodium carbonate (Na_2CO_3) were obtained from Caledon Laboratories Ltd. (Rockville, Ontario) and were used as received. 1-Ethyl-3-(3-dimethylaminopropyl)carbodiimide hydrochoride (EDC) and BupH 2-(*N*-morpholino)ethanesulfonic acid (MES) buffered saline packets were obtained from Pierce through Thermo Scientific (Rockford, IL) and were used as received or according to the package instructions. All deionized water was filtered to have a resistivity of 18.2 MΩ cm and was obtained from a Milli-Q Plus system from Millipore (Billerica, MA). Anhydrous ethanol was obtained from Commercial Alcohols (Brampton, Ontario). Glass cover slips were 25×25 mm and obtained from Fisher Scientific (Ottawa, Ontario). Cr and Au were 99.999% and obtained from ESPI (Ashland, OR). Au annealing was performed in a Thermolyne muffle furnace from Thermo Fisher Scientific (Ottawa, Ontario). Photographs of the films were taken with a Pentax K2000 DSLR camera fitted with a SMC Pentax-DA 1:2.8 35-mm rectilinear macro lens. Image processing of the photographs was performed using Picasa 3 (Google, Menlo Park, CA).

Microgels and etalons were prepared as previously described [13–15, 28–30]. Microgels of three different diameters were used for the current study, and they will be annotated as pNIPAm-*co*-AAc-1 (large diameter), pNIPAm-*co*-AAc-2 (medium diameter), and pNIPAm-*co*-AAc-3 (small diameter) throughout the text. The microgels had a hydrodynamic diameter of 1547.8 (±15.8 nm), 659.3 (±9.9 nm), and 229.0 nm (±4.6 nm), respectively, as measured by photon correlation spectroscopy. Specific details for the microgel syntheses and characterization can also be found in the Electronic Supplementary Material.

APBA functionalization of microgel thin films Functionalization of microgels with APBA was performed on a set of microgel films on gold similar to previously published procedures [17, 18]. All reagents were used in excess to ensure complete conversion of the acrylic acid moieties in the microgels to APBA functional groups.

Briefly, pNIPAm-*co*-AAc microgel thin films (for the three sizes of microgels) were painted onto a 15 nm Au gold-coated glass cover slip (2 nm Cr adhesion layer) to create a homogeneous, monolithic film [29, 30]. The films were soaked overnight in deionized water to remove any non-specifically adsorbed microgels. The microgel films were placed in pH 4.7 MES buffered saline (Pierce, prepared according to the packet instructions) and 9 mg APBA was added to the buffer. The solution and sample were allowed to mix for 1 h on a Gyratory Water Bath Shaker G76 (Brunswick Scientific Co., New Brunswick, NJ). To the mixture and sample, 20 mg EDC was added to the buffered APBA solution and sample. The mixture was swirled to dissolve the EDC, and the sample was placed into the refrigerator for 5 h. An additional 4.5 mg of APBA was added per sample to the solution and the mixture was allowed to mix on a gyrating shaker table for 30 min. Then an additional 20 mg per sample of EDC was added and dissolved, and the reaction was allowed to go overnight at 4 °C.

Control samples were made as above using pNIPAm-*co*-AAc microgel films treated with either APBA only or EDC only in pH 4.7 buffer. A set of double controls was made as above using NIPAm-BIS microgels *without* an AAc comonomer by adding APBA and EDC, as well as APBA only and EDC only.

All samples were rinsed with deionized water and soaked in pH 7.2 10 mM PBS buffer (with 150 mM ionic strength from NaCl) for several hours to remove any unreacted reagents. The samples were rinsed with H_2O and dried and placed into a gold evaporation apparatus (Torr International Inc. model THEUPG thermal evaporation system, New Windsor, NY) and 2 nm Cr (adhesion layer) and 5 nm Au was evaporated onto the functionalized films at a rate of 1 and 0.2 Å s^{-1}, respectively. The completed etalons were soaked in deionized H_2O. Prior to analysis, the etalons were rinsed and placed in pH 9 carbonate buffer for storage.

Glucose buffer preparation A 5-mM pH 9 carbonate buffer was prepared by dissolving 0.76 g $NaHCO_3$ and 0.11 g Na_2CO_3 in 2 L deionized H_2O in a volumetric flask [32]. The resulting solution measured pH 9.3. To prepare the glucose buffer, 3.0 g of α-D-glucose was dissolved in 500 mL of 5 mM pH 9 carbonate buffer to give a 6 mg/mL glucose solution. The final pH was 9.3.

Determination of etalon glucose responsivity Each sample was measured for thermoresponsivity in 24 mL of pH 9 buffer in a temperature controlled chamber fitted with a UV/vis reflectance probe from Ocean Optics (Dunedin, FL). The sample and buffer were cooled to 15 °C and the temperature was changed manually by increasing in increments of 3 °C up to 39 °C. The temperature was allowed to stabilize for 5 min at each temperature before a spectrum was recorded.

After the initial temperature study, the sample was cooled back to 15 °C. Approximately 12 mL of the pH 9 carbonate buffer was removed from the temperature controlled chamber using a glass syringe and was replaced with a cooled solution of 6 mg/mL glucose in pH 9 carbonate buffer, resulting in a final concentration of 3 mg/mL glucose in the chamber. Once the glucose was introduced, a spectrum

was recorded every 1 min using Ocean Optics Spectra Suite Spectroscopy Software (Dunedin, FL) for 2 h. Following equilibration with glucose, the temperature responsivity was measured again in the same manner as above keeping the sample in the glucose solution.

Atomic force microscopy imaging In-liquid height analysis for a pNIPAm-*co*-AAc-2 microgel etalon in 5 mM carbonate buffer, pH 9 and 3 mg/mL glucose in pH 9 buffer solution was performed using the APBA-functionalized and the APBA-exposed control samples used in this study. The images were acquired using an Asylum Research MFP 3D AFM (Santa Barbara, CA). Images were acquired over a 50×50-μm area using a scan rate of 0.45 Hz, using 512 scan points and lines. The tips were Olympus TR800PSA with a resonant frequency of 24 kHz. An image was taken using a sessile drop method first in pH 9 carbonate buffer at ~24 °C. The samples were treated with 3 mg/mL glucose solution for at least 2 h in a cooler with ice to approximate the binding conditions used in the experiments above. Then the samples were imaged in a sessile drop of 3 mg/mL glucose in pH 9 buffer at an ambient chamber temperature of ~24 °C. For this analysis, a line was scratched into the sample using a new razor blade and the scratch was imaged. The height was determined using the software by taking 100-line blocks and measuring the height on a line trace. Four 100-line blocks were measured and averaged to get an average height and standard deviation for each image (Electronic Supplementary Material).

Results and discussion

Functionalization of microgels in solution can be difficult due to aggregation and destabilization of the colloid as a result of a change in the surface charge density, and a concomitant change in the interaction potential of the microgels. Therefore, functionalization of the microgels for these studies was performed on the painted films before Au overlayer addition. First, the microgels were painted onto a 15 nm Au (with 2 nm Cr adhesion layer) base layer on glass, rinsed with H_2O and soaked in H_2O overnight to remove any non-specifically adsorbed microgels [29]. The microgel films were then subjected to functionalization in pH 4.7 MES buffer with EDC and APBA (Fig. 1a). Etalon fabrication was completed by adding a 5-nm Au overlayer to the functionalized films (with 2 nm Cr adhesion layer). After rehydrating the films in water and then in 5 mM pH 9 carbonate buffer, the devices were ready for analysis.

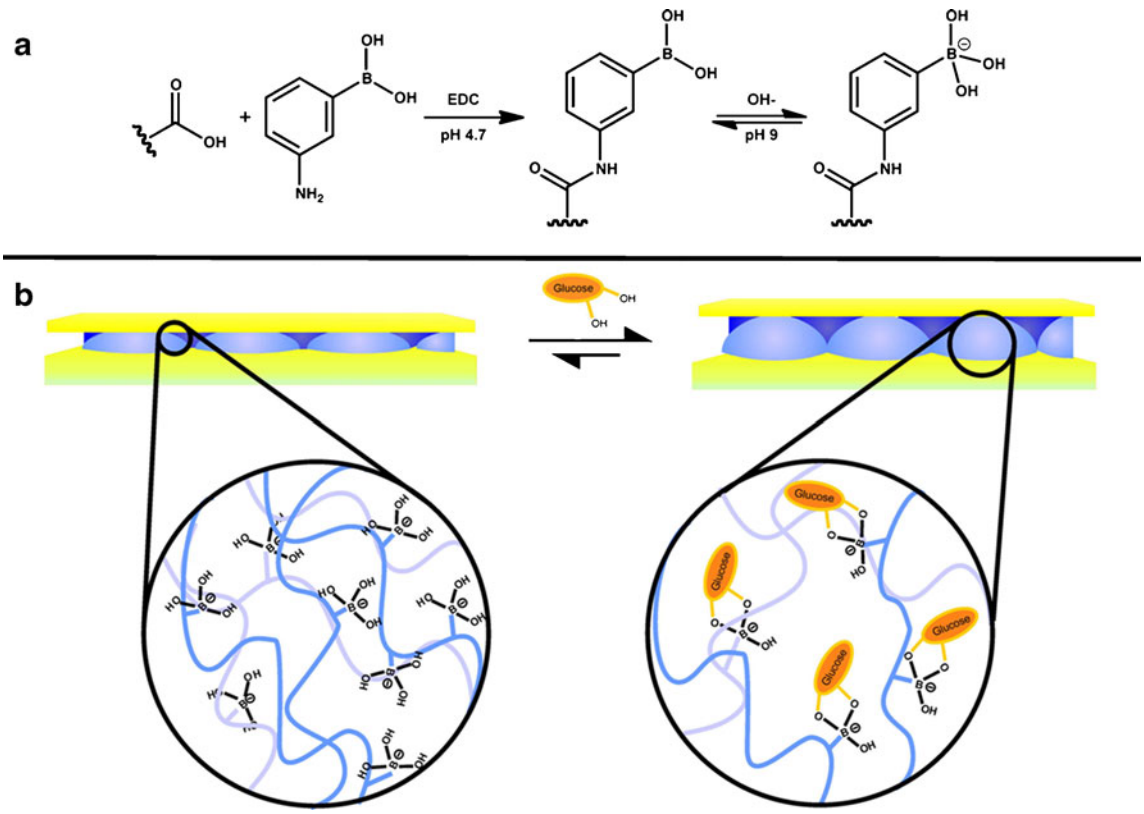

Fig. 1 Reaction scheme for (**a**) the functionalization of the acrylic acid moieties on the microgel with 3-aminophenylboronic acid (APBA) followed by the activation of the boronic acid with base and (**b**) a cartoon depiction of the glucose responsivity of an APBA-functionalized microgel etalon at pH 9

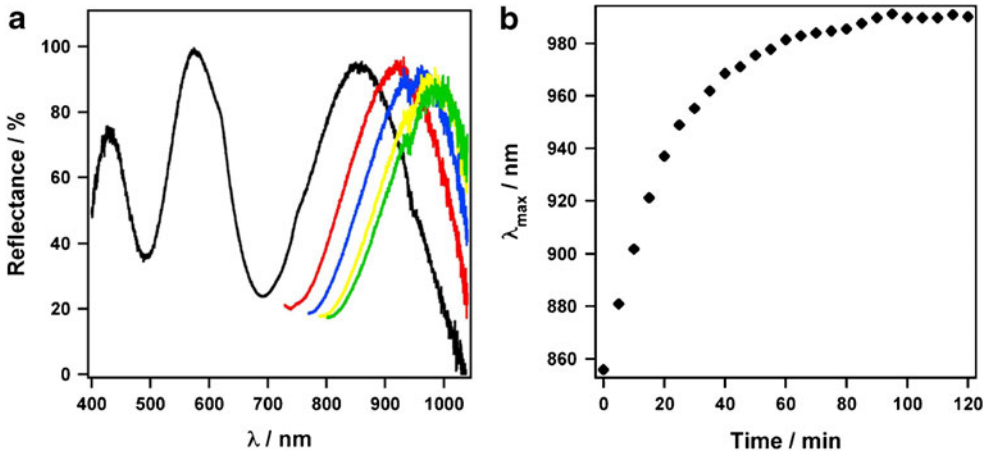

Fig. 2 Glucose responsivity shown as (**a**) a shift in the spectrum for the pNIPAm-*co*-AAc-2 microgel etalon and (**b**) as a function of time based on the peak position of the most red-shifted peak in (**a**). For panel (**a**), the *black trace* is the initial spectrum, in addition to truncated spectra for the most red-shifted peak as a function of time after glucose introduction: (*red*) 15, (*blue*) 30, (*yellow*) 60, and (*green*) 120 min. In (**b**), the peak position for the most red-shifted peak is plotted as a function of time after glucose introduction. Total spectral shift is 134 nm

The analysis of the glucose sensitive materials was performed in 5 mM pH 9 carbonate buffer. In a basic buffer the boronic acid moieties on the APBA (pK_a=8.2 [17, 33])were hydroxylated such that the boron possesses a negative charge (Fig. 1) [17, 18, 33, 34]. The binding for diols, like glucose, is favored for boronic acids in the charged state [34]. As glucose binds, more boronic acid groups must convert to the charged state in order to maintain the equilibrium, which effective lowers the pK_a. As more boron atoms become charged, more glucose can bind until equilibrium is reached [18]. In the presence of glucose, the bound state is preferred promoting more hydroxylation of the boron atoms into a charged form, leading to an increase in the Coulombic repulsion inside the microgel, which results in a swelling response. In the etalons this will be observed as a red shift, according to Eq. 1. Previous studies have shown that the change in the distance between the Au is more important for tuning of the etalon color than changes in the refractive index, *n* [28–30]. We are able to measure the binding of glucose directly using our etalons and observing the spectral shift that results from microgel swelling. We exposed the etalons to a 3 mg/mL solution of glucose in pH 9 carbonate buffer and observe changes in peak position in the etalon's spectrum as a function time. For pNIPAm-*co*-AAc-2 microgel etalons functionalized with APBA, we see a 134 nm spectral shift in the most red-shifted peak starting at 856 nm and ending at 990 nm (Fig. 2a) over the course of 2 h. When the peak position is plotted as a function of time (Fig. 2b), it becomes apparent that the majority of the spectral shift is observed within 30 min of glucose introduction, with an eventual leveling off as the boronic acid groups bind and reach an equilibrium with the available glucose. This observation is similar to other hydrogel sensing devices using boronic acid binding of glucose [6, 10, 11]. The controls that were exposed during fabrication to either APBA only or EDC only showed only minimal changes in the spectrum or peak position after the addition of glucose (Fig. 3). A double control was also performed using pNIPAm-BIS microgels that did not have any acrylic acid as a co-monomer. These microgels were treated in the same way as all of the samples containing acrylic acid using APBA and EDC. These microgels continued to

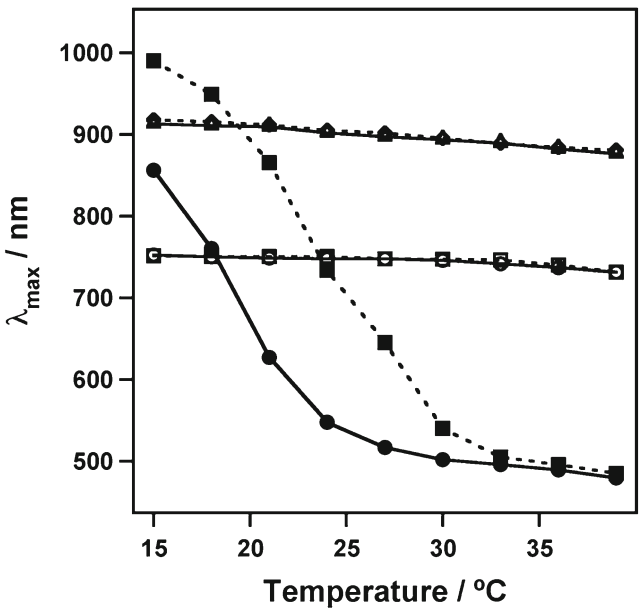

Fig. 3 A plot of the most red-shifted peak in the spectrum for the pNIPAm-*co*-AAc-2 microgel etalon as a function of temperature for the APBA-functionalized microgel etalons and two controls exposed to either APBA only or EDC only. The *black solid circles* show the VPTT curve for the APBA-functionalized microgels in 5 mM pH 9 carbonate buffer before the addition of glucose, while the *black solid squares* show the same etalon after glucose addition. The most red-shifted peaks of the APBA-only etalon (*open circles* and *open squares*) and EDC-only etalon (*open triangles* and *open diamonds*) controls are also plotted as a function of temperature before and after glucose addition, respectively

show responsivity to temperature even in the pH 9 carbonate buffer, but they also did not exhibit any shifts in the VPTT of the film nor responsivity after glucose exposure (Electronic Supplementary Material, Figure S1).

Prior to binding with glucose we measured the thermoresponsivity of the APBA-modified pNIPAm-*co*-AAc-2 microgel etalons (Fig. 3) in 5 mM pH 9 carbonate buffer. We measured the etalon's spectrum every 3 °C between 15 °C and 39 °C. When the most red-shifted peak position is plotted as a function of temperature we see that the behavior mimics previously studied microgels in solution (Fig. 3) [17, 18]. Native pNIPAm microgels in solution exhibit a VPTT of ~32 °C. The APBA etalons, however, exhibit an initial VPTT of ~18 °C with a total shift of ~400 nm in response to temperature. When Zhou and co-workers studied APBA-functionalized microgels in solution they reported a depressed VPTT of 17 °C [17]. This comparison is important to make, as it shows that microgel confinement does not affect their function. Zhou and co-workers attributed this to the increased hydrophobicity imparted to the microgels as a result of the APBA functional group. After exposure of the APBA-functionalized etalon to 3 mg/mL glucose solution in pH 9 carbonate buffer, the etalon's spectrum red shifts 134 nm. If the wavelength position of that shifted peak is again monitored as a function of temperature, an increase in the VPTT to 24 °C is observed. The VPTT for glucose-bound APBA-functionalized microgels in solution as reported by Zhou and co-workers is also 24 °C [17]. In our case, we see a total 6 °C shift in the VPTT, which is similar to the 7 °C shift seen by Zhou, as well as the 4 °C shift reported by Hoare and Pelton for APBA-functionalized microgels in solution [17, 18]. The shift of the VPTT is attributed to an increase in the charge density inside the particles causing Coulombic repulsion. The controls exposed to APBA only or EDC only do not exhibit any thermoresponsivity because the AAc groups have not been modified in any way (Fig. 3). At pH 9, the AAc groups are well above their pK_a and will all be negatively charged. In such cases, the Coulombic repulsion of the $-COO^-$ groups inside the gel will be enough to suppress the thermoresponsivity [13]. As mentioned above, the position of the control peaks changes minimally after glucose exposure. Therefore, after glucose exposure the response to temperature is still suppressed by the Coulombic repulsion of the AAc groups in the microgels.

Etalons made with larger and smaller microgels (pNIPAm-*co*-AAc-1 and pNIPAm-*co*-AAc-3, respectively) show a comparable response by: (a) exhibiting a red shift in the spectrum upon the addition of glucose and (b) exhibiting a shift in the VPTT before and after glucose addition (Fig. 4). The magnitude of the response of these etalons to glucose is very similar to the medium diameter pNIPAm-*co*-AAc-2 microgel etalons. Important to note is that all of the APBA-functionalized devices exhibit the majority of their response within 30 min of glucose introduction (Figs. 2 and 4b, e). This indicates that the binding is more affected by the binding equilibrium of the glucose with the boronic acid, rather than the incorporation of the analyte into the device. While it is the case that the majority of the response exhibited by each etalon occurs within 30 min of glucose introduction, the large diameter microgels do exhibit slower response kinetics, shifting an additional 35 nm overnight after the initial 2 h. In comparison, the medium and small microgels do not show any additional spectral shift after overnight incubation. The most notable difference between the etalons made from microgels of different size is that each of them produce spectra with different numbers of peaks where the smallest microgels give a single reflectance peak (Fig. 4d), and the largest gives five peaks (Fig. 4a). As expected, the medium diameter pNIPAm-*co*-AAc-2 microgels give an etalon that exhibits an intermediate number of spectral peaks (Fig. 1a). We have shown previously that the spectral properties can be tuned by changing the size and stiffness of the microgels in order to produce an etalon with a single reflectance color, both spectrally and visually [30]. These and other parameters, such as responsivity to specific analytes, will be crucial in directing design of these materials for real POC usage.

When the etalons are analyzed in the same manner as the pNIPAm-*co*-AAc-2 microgel etalons, the large diameter pNIPAm-*co*-AAc-1 microgels show an overall 150 nm shift in the spectrum due to glucose binding inside the film (Fig. 4a–c). Similarly, the small diameter microgel etalons show a 110 nm shift (Fig. 4d–f). As shown in Fig. 4c, for the pNIPAm-*co*-AAc-1 microgel etalons, the VPTT of the APBA-functionalized films is 18 °C, but shifts to 27 °C after incubation overnight in 3 mg/mL glucose. The etalons made with the small diameter microgels, pNIPAm-*co*-AAc-3, show a similar response with a VPTT of 20 °C before glucose addition that shifts to 26 °C after incubation with glucose (Fig. 4f). This is important because it shows that changing the microgel does not change the expected response and indicates that the spectral and visual color properties can be tuned without losing sensitivity.

Atomic force microscopy (AFM) imaging, and subsequent height analysis, shows that the APBA-functionalized pNIPAm-*co*-AAc-2 etalons exhibit a total change in d of (+)43 nm after the addition of glucose. At an ambient AFM chamber temperature of 24 °C, the etalons have a d of 340 nm (±9 nm). After incubating the etalon with 3 mg/mL glucose in pH 9 carbonate buffer for 2 h the total thickness increased to 383 nm (±5 nm). If we assume that we are looking at a first order peak for these materials [30], we can use Eq. 1 to calculate the expected total change in d that should yield the observed $\Delta\lambda$. Assuming a refractive index of 1.4, and a first order peak, the $\Delta\lambda$ should be (+)

70 nm at 24 °C. This calculated value closely matches the actual change in *d*, indicating that our etalon functions as expected. The control exposed to APBA only during fabrication did not show a significant change in thickness by AFM before and after glucose addition, as expected. The APBA-only etalon was 777 nm (±10 nm) thick before reaction with glucose and 787 nm (±27 nm) thick after reaction with glucose. Actual AFM images are in Electronic Supplementary Material, Figure S2.

Ultimately, we hope to use these materials as visual readout sensor devices for POC diagnostics, similar to a pregnancy test or a glucose monitor. In Fig. 5, we show photographs of the etalons used in the spectral experiments as a proof of concept. Figure 5a, b shows pictures of the APBA-functionalized pNIPAm-*co*-AAc-2 microgel etalon before and after glucose addition, respectively. While the color change is subtle, it is visibly detectable, and the entire etalon exhibits a complete color reversal going from mostly green at pH 9 as shown in Fig. 5a, to mostly red in a 3 mg/mL glucose solution as shown in Fig. 5b. The controls in Fig. 5c–f do not show any significant differences before and after glucose addition further indicating that the addition of glucose does not change their properties significantly enough to elicit a colorimetric response.

Conclusions

We have demonstrated that microgel etalons are good platforms for sensing applications by using them to spectrally and

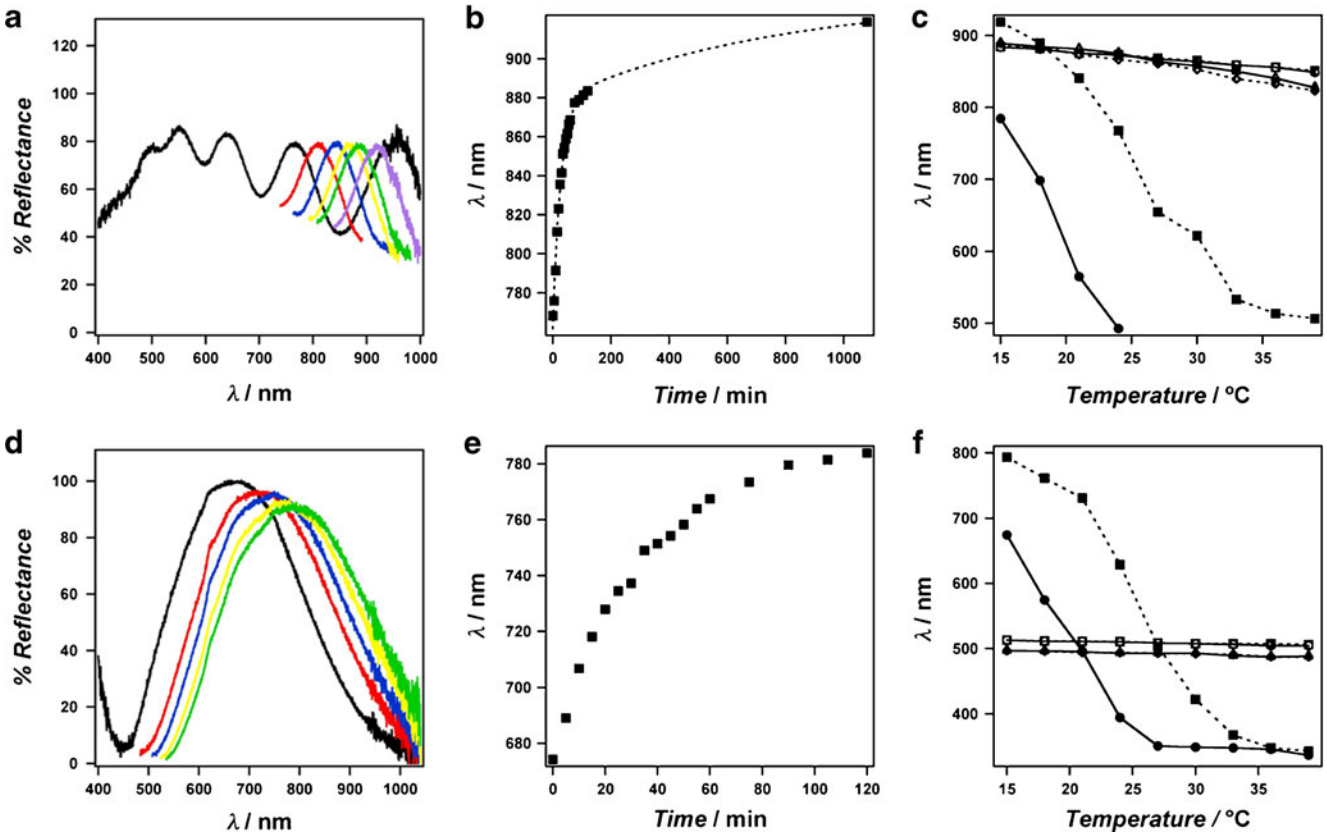

Fig. 4 Glucose responsivity for the large diameter pNIPAm-*co*-AAc-1 microgels as (**a**) a shift in the spectrum for the film, (**b**) as a function of time based on the peak position of the second red-shifted peak in (**a**) (λ_0=758 nm), and (**c**) as a function of the effect of glucose on the VPTT. Glucose responsivity is also shown for the small diameter pNIPAm-*co*-AAc-3 microgels as (**d**) a shift in the spectrum for the film, (**e**) as a function of time based on the peak position in (**d**), and (**f**) as a function of the effect of glucose on the VPTT. For panel (**a**), the *black trace* is the initial spectrum, in addition to truncated spectra for the most red-shifted peak, (*red*) 15, (*blue*) 30, (*yellow*) 60, and (*green*) 120 min, and (*purple*) overnight (approximately 18 h) following glucose addition. In (**b**), the peak position for the second red-shifted peak is plotted as a function of time after glucose introduction; the *dashed line* is drawn to guide the eye. Total spectral shift is 151 nm. For panel (**d**), the *black trace* is the initial spectrum, in addition to truncated spectra as a function of time after glucose introduction: (*red*) 15, (*blue*) 30, (*yellow*) 60, and (*green*) 120 min. In (**e**), the peak position for the peak is plotted as a function of time after glucose introduction; the *dashed line* is drawn to guide the eye. Total spectral shift is 110 nm. Panels (**c**) and (**f**) show the APBA-functionalized microgel etalons and two controls exposed to either APBA only or EDC only. The *black solid circles* show the VPTT curve for the APBA-functionalized microgels in 5 mM pH 9 carbonate buffer before the addition of glucose, while the *black solid squares* show the same etalon after glucose addition. The most red-shifted peaks of the APBA-only etalon (*open circles* and *open squares*) and EDC-only etalon (*open triangles* and *open diamonds*) controls are also plotted as a function of temperature before and after glucose addition, respectively

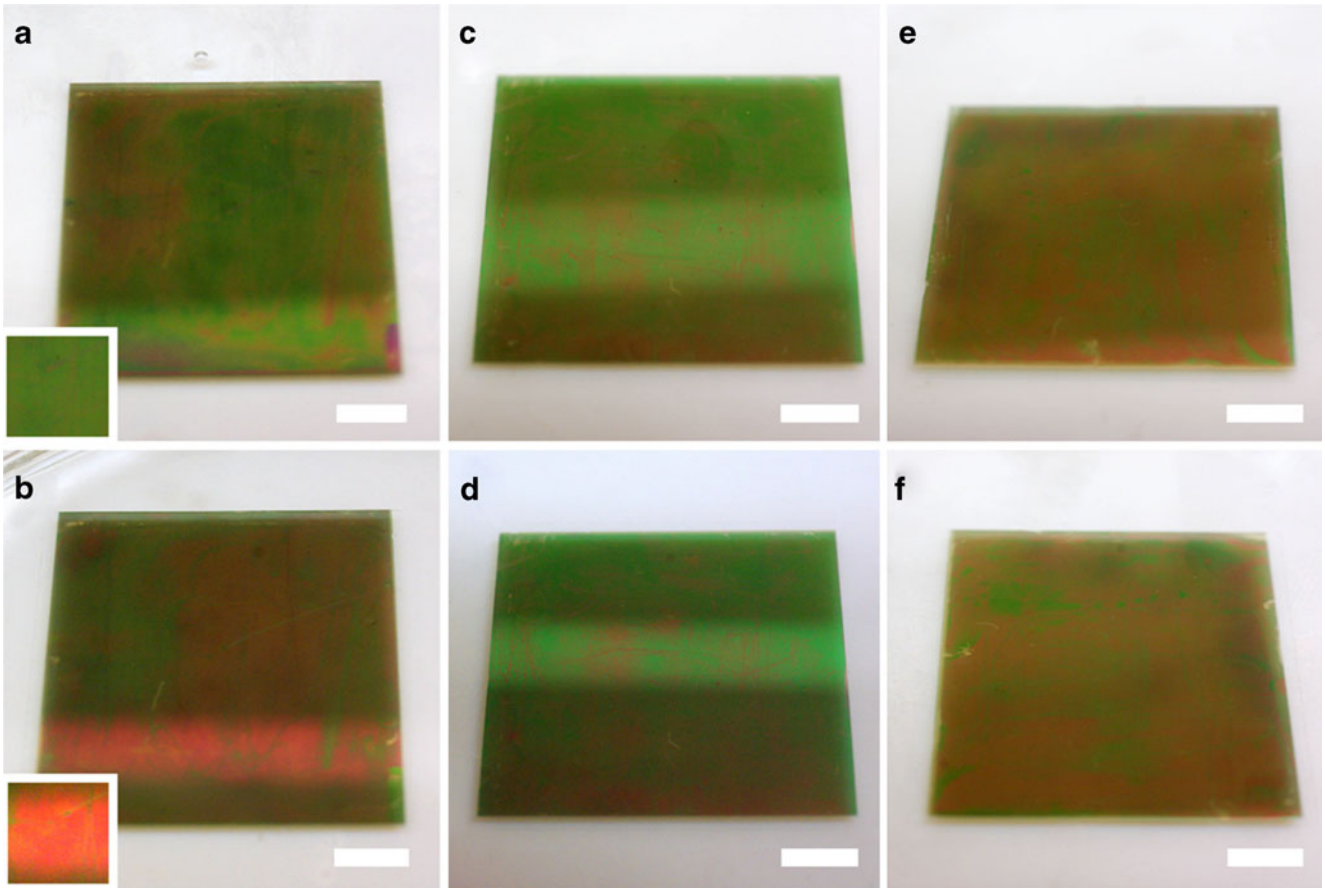

Fig. 5 APBA-functionalized microgel etalons are *green* (**a**) before glucose addition, but change to *red* (**b**) after glucose addition. The etalons fabricated by exposure to APBA only show no significant change in color (**c**) before and (**d**) after glucose exposure. Similarly, the etalons exposed to EDC only show no significant color change (**e**) before and (**f**) after glucose exposure. *Insets* show a cropped image of the approximate center 1 cm^2 of each etalon. To make the etalon's color more apparent, the image brightness of the select region of the etalon was increased using image processing software. *Scale bars* are 5 mm

visually detect glucose in aqueous solution. Functionalization of microgels at an interface is a reasonable alternative to functionalization of microgels in solution, which may result in irreversible aggregation. The surface-functionalized microgels exhibit similar behavior to that seen by previous investigators for microgels in solution [18]. In response to glucose, APBA-functionalized microgel etalons exhibit 110–150 nm red shift in response to a 3 mg/mL glucose solution in 5 mM pH 9 carbonate buffer at 15 °C. Additionally, before binding with glucose the etalons exhibit a VPTT of 18–20 °C, which shifts to 24–26 °C after glucose addition. Etalons with microgels of different sizes give similar responses, the most marked difference being the different numbers of spectral peaks exhibited by each. We further demonstrated that the visual color shift of the device is significant enough to show a clear change in color from green to red before and after the addition of glucose, respectively. These experiments clearly demonstrate microgels etalons' utility for future sensing applications. While glucose sensitive microgels are known, their glucose response needs to be determined via light scattering intensity changes or diameter changes measured via photon correlation spectroscopy [17, 18]. Using the device presented here, their response can simply be read out visually and spectrally if needed. It should also be pointed out that the microgels themselves are thermoresponsive, therefore the material's color can be significantly influenced by temperature. For POC applications, this is a concern. In the future, we will develop arrayed sensors that will contain control etalons on a single substrate, along with the test etalon, such that the temperature effect can be negated.

Acknowledgments M.J.S. acknowledges funding from the University of Alberta (the Department of Chemistry and the Faculty of Science), the Natural Science and Engineering Research Council (NSERC), the Canada Foundation for Innovation (CFI), and the Alberta Advanced Education & Technology Small Equipment Grants Program (AET/SEGP). M.J.S acknowledges Prof. Mark McDermott for the use of the thermal evaporator and Dr. Ryan Fuierer (Asylum Research) for providing AFM tips. Prof. Ravin Narain is acknowledged for the use of the dynamic light scattering instrument and the Alberta Centre for Surface Engineering and Science (ACSES) is acknowledged for the AFM use.

References

1. Yager P, Domingo GJ, Gerdes J (2008) Point-of-care diagnostics for global health. Annu Rev Biomed Eng 10:107–144
2. Mabey D, Peeling Rosanna W, Ustianowski A, Perkins Mark D (2004) Diagnostics for the developing world. Nat Rev Microbiol 2 (3):231–240
3. Tudos AJ, Besselink GJ, Schasfoort RB (2001) Trends in miniaturized total analysis systems for point-of-care testing in clinical chemistry. Lab on a chip 1(2):83–95
4. Delouise LA, Fauchet PM, Miller BL, Pentland AA (2005) Hydrogel-supported optical-microcavity sensors. Adv Mater 17: 2199–2203
5. Bonanno LM, DeLouise LA (2010) Integration of a chemical-responsive hydrogel into a porous silicon photonic sensor for visual colorimetric readout. Adv Funct Mater 20(4):573–578
6. Alexeev VL, Sharma AC, Goponenko AV, Das S, Lednev IK, Wilcox CS, Finegold DN, Asher SA (2003) High ionic strength glucose-sensing photonic crystal. Anal Chem 75(10):2316–2323
7. Norman RJ, Lowings C, Chard T (1985) Dipstick method for human chorionic gonadotropin suitable for emergency use on whole blood and other fluids. Lancet 1(8419):19–20
8. Chan S, Horner SR, Fauchet PM, Miller BL (2001) Identification of Gram negative bacteria using nanoscale silicon microcavities. J Am Chem Soc 123(47):11797–11798
9. Chan S, Fauchet PM, Li Y, Rothberg LJ (2000) Nanoscale microcavities for biomedical sensor applications. Proceedings of SPIE-The International Society for Optical Engineering 3912 (Micro- and Nanotechnology for Biomedical and Environmental Applications):23–34
10. Ward-Muscatello MM, Stunja LE, Asher SA (2009) Polymerized crystalline colloidal array sensing of high glucose concentrations. Anal Chem 81(12):4978–4986
11. Asher SA, Alexeev VL, Goponenko AV, Sharma AC, Lednev IK, Wilcox CS, Finegold DN (2003) Photonic crystal carbohydrate sensors: low ionic strength sugar sensing. J Am Chem Soc 125 (11):3322–3329
12. Holtz JH, Asher SA (1997) Polymerized colloidal crystal hydrogel films as intelligent chemical sensing materials. Nature 389:829–832
13. Jones CD, Lyon LA (2000) Synthesis and characterization of multi-responsive core-shell microgels. Macromolecules 33(22):8301–8306
14. Serpe MJ, Jones CD, Lyon LA (2003) Layer-by-layer deposition of thermoresponsive microgel thin films. Langmuir 19(21):8759–8764
15. Meng Z, Smith MH, Lyon LA (2009) Temperature-programmed synthesis of micron-sized multi-responsive microgels. Colloid Polym Sci 287(3):277–285
16. Kim J, Singh N, Lyon LA (2006) Label-free biosensing with hydrogel microlenses. Angew Chem Int Edit 45(9):1446–1449
17. Zhang Y, Guan Y, Zhou S (2006) Synthesis and volume phase transitions of glucose-senstive microgels. Biomacromolecules 7:3196–3201
18. Hoare T, Pelton R (2007) Engineering glucose swelling responses in poly(*N*-isopropylacrylamide)-based microgels. Macromolecules 40:670–678
19. Kataoka K, Miyazaki H, Bunya M, Okano T, Sakurai Y (1998) Totally synthetic polymer gels responding to external glucose concentration: their preparation and application to on–off regulation of insulin release. J Am Chem Soc 120:12694–12695
20. Sorrell CD, Lyon LA (2008) Deformation controlled assembly of binary microgel thin films. Langmuir 24:7216–7222
21. South AB, Whitmire RE, Garcia AJ, Lyon LA (2009) Centrifugal deposition of microgels for the rapid assembly of nonfouling thin films. ACS Appl Mater Interfaces 1(12):2747–2754. doi:10.1021/am9005435
22. Serpe MJ, Lyon LA (2004) Optical and acoustic studies of pH-dependent swelling in microgel thin films. Chem Mater 16(22): 4373–4380
23. Sorrell CD, Lyon LA (2007) Bimodal swelling responses in microgel thin films. J Phys Chem B 111(16):4060–4066
24. Tsuji S, Kawaguchi H (2005) Colored thin films prepared from hydrogel microspheres. Langmuir 21(18):8439–8442
25. Zhou M, Xing F, Ren M, Feng Y, Zhao Y, Qiu H, Wang X, Gao C, Sun F, He Y, Ma Z, Wen P, Gao J (2009) A facile method to assemble PNIPAM-containing microgel photonic crystals. ChemPhysChem 10 (3):523–526
26. Vaughan JM (1989) The Fabry–Perot Interferometer: history, theory, practice and applications. In: Pike ER, Welford WT (eds) Optics and optoelectronics. Taylor & Francis Group, New York, p 583
27. Brooker G (2003) Modern classical optics. In: Atomic, optical, and laser physics. Oxford University Press, Oxford, p 397
28. Sorrell CD, Carter MCD, Serpe MJ (2011) Color tunable poly (*N*-isopropylacrylamide)-co-acrylic acid microgel–Au hybrid assemblies. Adv Funct Mater 21(3):425–433
29. Sorrell CD, Carter MCD, Serpe MJ (2011) A "paint-on" protocol for the facile assembly of uniform microgel coatings for color tunable etalon fabrication. ACS Appl Mater Interfaces 3:1140–1147
30. Sorrell CD, Serpe MJ (2011) Reflection order selectivity of color-tunable poly (*N*-isopropylacrylamide) microgel based etalons. Adv Mater 23:4088–4092
31. Carter MCD, Sorrell CD, Serpe MJ (2011) Deswelling kinetics of color tunable poly (*N*-isopropylacrylamide) microgel based etalons. J Phys Chem B 115:14359–14368
32. Delory GE, King EJ (1945) A sodium carbonate–bicarbonate buffer for alkaline phosphatases. Biochem J 39:16
33. Matsumoto A, Yoshida R, Kataoka K (2004) Glucose-responsive polymer gel bearing phenylborate derivative as a glucose-sensing moiety operating at the physiological pH. Biomacromolecules 5:1038–1045
34. Springsteen G, Wang B (2002) A detailed examination of boronic acid–diol complexation. Tetrahedron 58:5291–5300